ULTRASONIC ESTIMATION OF MECHANICAL PROPERTIES OF PULMONARY ARTERIAL WALL UNDER NORMOXIC AND HYPOXIC CONDITIONS[*]

Kendall R. Waters[1] and Osama M. Mukdadi[2]

[1]National Institute of Standards and Technology, Materials Reliability Division, Boulder, Colorado, 80305 USA
[2]The Children's Hospital, University of Colorado Health Sciences Center, Denver, Colorado, 80218 USA

ABSTRACT. Secondary pediatric pulmonary hypertension is a disease that could benefit from improved ultrasonic diagnostic techniques. We perform high-frequency *in vitro* ultrasound measurements (25 MHz to 100 MHz) on fresh and fixed pulmonary arterial walls excised from normoxic and hypoxic Long-Evans rat models. Estimates of the elastic stiffness coefficients are determined from measurements of the speed of sound. Preliminary results indicate that hypoxia leads to up to increase of 20 % in stiffening of the pulmonary arterial wall.

INTRODUCTION

Motivation

Secondary pulmonary hypertension (PHT) is a potentially fatal complication of congenital heart defects in children, particularly those who live at high altitude. Discovering the pathophysiology and expression of the disease may lead to improved diagnostics and treatments. We investigate how the ultrasonic and mechanical properties of the healthy tissues of the pulmonary artery and its constituents differ from those of diseased tissue.

The reduced oxygen content in high-altitude environments causes children born with heart defects to have a greater propensity for developing PHT. A long-term goal of the current research is to develop less invasive diagnostics that might hasten treatment and mitigate permanent damage. At present, diagnosis is sometimes delayed by two factors: a variety of pathological conditions can display similar clinical expression, and physicians are reluctant to subject a child to catheterization unless it is clearly necessary, because it is an invasive technique [1]. Consequently, a need exists for improved understanding of the ultrasonic and elastic properties of the wall of the pulmonary artery (PA).

Our goal is to quantitatively evaluate mechanical properties of normoxic (having normal oxygen content) and hypoxic (having reduced oxygen content) pulmonary arteries and identify structural differences between these populations. We begin with an animal model. The Long-Evans breed of rats is chosen because it can be genetically modified so that the endothelin B receptor is disabled. The endothelin B receptor is responsible for activating vasodilators, which play a role in how an arterial wall responds to changes in the mechanical stress environment. A low-pressure, reduced-oxygen environment is used to induce PHT.

STRUCTURE AND ELASTIC PROPERTIES OF PULMONARY ARTERY

The elevated blood pressure in the PA in patients that suffer from secondary PHT leads to a stiffening of the PA that causes the heart to work harder, leading to still higher pressures. It is necessary to know both the structure of the PA, and how it remodels due to changes in the stress environment.

Pulmonary Artery

Figure 1(a) shows a cut-away illustration of an artery. It is the intima, which is in contact with the blood of the lumen, the media (M) that provides most of the elastic properties of an artery, and the adventitia (A). For purposes of the present study, we are interested primarily in the media. Figure 1(b) shows an optical micrograph of a histologic slice of the PA wall from a hypoxic rat model. It has been stained with Pentachrome to facilitate identification of certain cellular constituents. The 100 µm scale bar gives a sense of size to these structures. Constituents of normal media include smooth muscle (46 %), collagen (28 %), ground substance (17 %), and elastin (9 %) [2].

Remodeling due to Hypertension

Cells and tissues naturally develop in a mechanically stressed environment. Changes in the stress environment can lead to a number of structural and functional changes, including changes in mass and internal structure as well as the building or reabsorption of extracellular structures [2]. This may also modify the mechanical properties of the structure. In the case of hypertension, studies have shown that arteries remodel in order to normalize the associated increase in stress. Possible types of remodeling include thickening of media and adventitia and stiffening of the arterial wall. Here, thickening could be due to smooth muscle cell hypertrophy and increased collagen and elastin content.

(a)   **(b)**
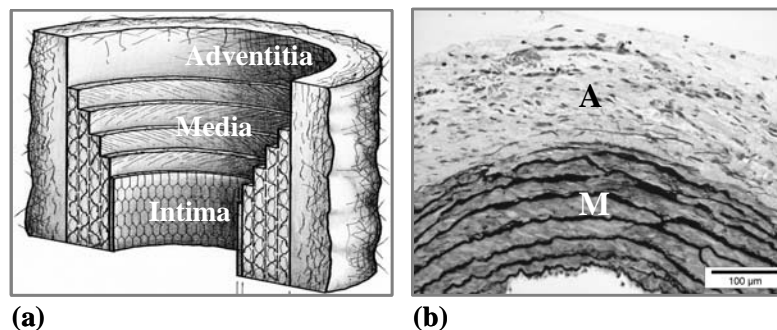
FIGURE 1. (a) Cut-away illustration of an artery. (b) Optical micrograph of a histologic slice of the pulmonary arterial wall from a hypoxic rat model stained with Pentachrome. A 100 µm scale bar is also included.

Elastic Symmetry

The medial layer of an artery is sometimes modeled as having orthotropic symmetry, with elastin fibers wrapping around the wall [3], such that there are nine independent elastic stiffness coefficients. The size of the rat model arteries and the current experimental measurement system limit the number of coefficients of tissue with orthotropic symmetry that we can measure. Consequently, we have chosen to approximate the medial layer as being transversely isotropic, with only 5 independent elastic stiffness coefficients [4], as given by

$$
\begin{bmatrix}
c_{11} & c_{12} & c_{12} & 0 & 0 & 0 \\
c_{12} & c_{22} & c_{12} & 0 & 0 & 0 \\
c_{12} & c_{12} & c_{33} & 0 & 0 & 0 \\
0 & 0 & 0 & c_{44} & 0 & 0 \\
0 & 0 & 0 & 0 & \frac{c_{11}-c_{13}}{2} & 0 \\
0 & 0 & 0 & 0 & 0 & c_{44}
\end{bmatrix}
\tag{1}
$$

where the off-diagonal elements (c_{12}) are approximated as being equal. Measurements in the plane of the media permit determination of c_{11}, c_{22}, and c_{12}. Measurements through the thickness (out-of-plane) of the media permit determination of c_{33}. Last, we estimate c_{44} from values available in the literature, as discussed below. An illustration of the medial layer and the corresponding coordinate system is shown in Figure 2(a).

EXPERIMENTAL TECHNIQUE

Tissue Specimens and Preparation

The Long-Evans rat models are raised at the University of Colorado Health Sciences Center (UCHSC) in Denver. The rat models are sacrificed at 12 –13 weeks of age, and the extrapulmonary system (main trunk, left and right branches) is excised. The PAs are kept frozen (0 °C) until measurements are performed at the NIST facilities. The tissue is considered fresh if measured within 24 hours of sacrifice.

(a)   **(b)**
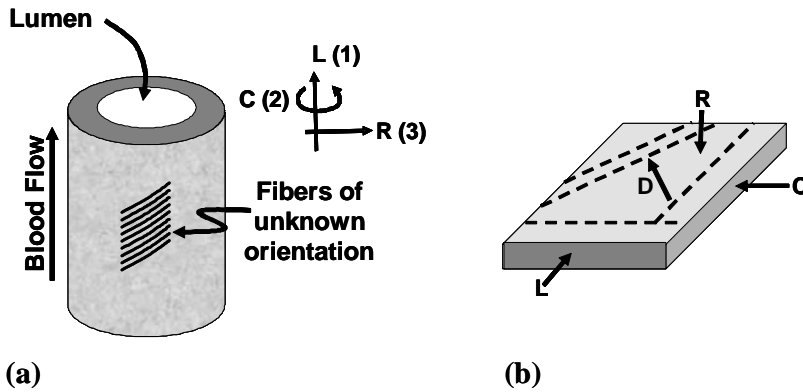
FIGURE 2. (a) Illustration of the medial layer with fibers of unknown orientation. Here, L (1) is the longitudinal direction, C (2) is the circumferential direction, and R (3) is the radial direction. (b) Illustration of tissue membrane and directions of measurement.

Three populations of rat models are considered: six normoxic Long-Evans (controls), four hypoxic Long-Evans, seven genetically modified (GM) hypoxic Long-Evans. The hypoxic rat models are placed for three weeks in a hypobaric chamber that simulates an altitude of 5200 m. This altitude has roughly half the oxygen content of air at sea level, such that the hypoxia presumably induces PHT.

The extrapulmonary system is further prepared prior to ultrasonic measurements. Each arterial section (left branch, right branch, main trunk) is segmented, and the PA wall is cut in the longitudinal direction. The artery wall is opened as a membrane, and adventitia is removed under an optical microscope by means of tissue scissors. Measurements on fresh tissue are performed in the out-of-plane direction (R) only. Following measurements of fresh tissue, specimens are placed in a fixative solution. Fixed tissue specimens are then used for measurements in the plane of the arterial wall (Figure 2b). Here the diagonal direction (D) is at 45° with respect to the longitudinal and circumferential directions.

Acoustic Microscope

Ultrasonic measurements are performed by use of an acoustic microscope (Figure 3). A 50 MHz transducer (6 mm diameter, 13 mm focal length, -6 dB bandwidth of 25 MHz to 65 MHz) is used for measurements of fresh tissue. A 100 MHz transducer (3 mm diameter, 6 mm focal length, -6 dB bandwidth of 55 MHz to 118 MHz) is used for measurements of fixed tissue because the beam diameter ($\approx$ 40 µm) is small compared to the PA wall thickness ($\approx$ 200 µm). Fresh tissue specimens are mounted on a stainless steel fixture and immersed in a degassed, nutritive solution heated to 37 °C. Similar measurements are performed on fixed tissue specimens except that deionized water is used. Motion control and data acquisition are automated.

Measurement Protocol

A standard double-transmission technique is employed such that the ultrasound propagates through the tissue from the transducer to the reflector and again from the reflector back to the transducer. The nominal focal plane of the transmitting transducer is at the stainless steel reflector. Reference scans are performed that include only the immersion fluid in the propagation path. The PA tissue is then substituted into the propagation path. Scans in the out-of-plane direction (R) of the PA wall are performed over an area of 2 mm $\times$ 3 mm with
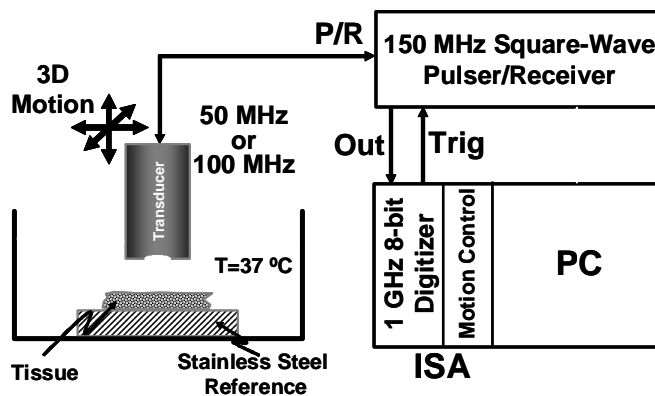
FIGURE 3. Schematic diagram of acoustic microscope.
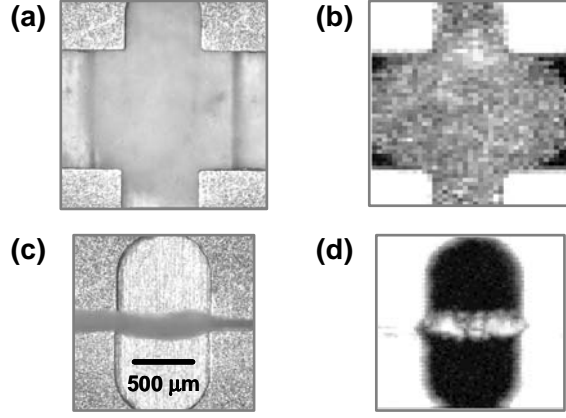
FIGURE 4. Comparison of optical micrographs (a,c) and acoustic amplitude C-Scans (b,d) of pulmonary artery measurements in the out-of-plane (a,b) and in-plane (c,d) directions. A 500 μm scale is included in (c).

a step size of 50μm. Scans in the plane of the PA wall are typically over an area of 1.5 mm × 1.5 mm with a step size of 20 μm. (See Figure 4.) The ultrasonic radio-frequency (RF) signals are saved to disk at each site for off-line analysis.

DATA REDUCTION

Analysis is performed at each measurement site in a selected region of interest (ROI) that is generally positioned in the center of the tissue specimen. The ROI for the out-of-plane measurements was approximately 0.5 mm × 0.5 mm (10 points × 10 points), and the ROI for the in-plane measurements was approximately 0.2 mm × 0.1 mm (10 points × 5 points).

Time-Domain Analysis

Speed of sound (SOS) in the PA tissue is determined from the changes in times of flight of the envelopes of the ultrasonic RF signals between the reference and tissue paths [5]:

$$v_{PA} = v_w \left(1 + \frac{\Delta t_{Shadowing}}{\Delta t_{PA}} \right), \tag{2}$$

where v_{PA} is the speed of sound in the PA wall, v_w is the temperature-dependent SOS in deionized water [6] or a nutrative solution, $\Delta t_{Shadowing}$ is the change in time-of-flight between the shadowed and unshadowed reflector, and Δt_{PA} is the time of flight through the PA tissue.

Ultrasonic Estimation of Elastic Properties

The elastic stiffness coefficients c_{11}, c_{22}, and c_{33}, and c_{12} are determined by use of standard relations between the stiffness and SOS for a transversely isotropic material [4]:

$$c_{11} = \rho v_L^2 \tag{3}$$
$$c_{22} = \rho v_C^2 \tag{4}$$
$$c_{33} = \rho v_R^2 \tag{5}$$

$$c_{12} = \left\{ \frac{\left(c_{11}\cos^2\vartheta + c_{44}\sin^2\vartheta\right)\left(c_{11}\sin^2\vartheta + c_{44}\cos^2\vartheta\right) - \rho v_D^2\left(c_{22}\sin^2\vartheta + c_{11}\cos^2\vartheta + c_{44}\right) + \rho^2 v_D^4}{|\sin\vartheta|/|\cos\vartheta|} \right\}^{\frac{1}{2}} - c_{44} \, , \quad (6)$$

where $\rho = 1060$ kg/m^3, $\vartheta = 45°$, $c_{44} = 0.1$ GPa [7], and v_L, v_C, v_R, and v_D are respectively the experimentally measured speeds of sound in the longitudinal, circumferential, radial, and diagonal directions determined by use of Eq. (2).

RESULTS AND DISCUSSION

Fresh Specimens

Measurements of the radial stiffness of the fresh PA walls for the three rat model populations are shown in Figure 5. The stiffnesses for the PA sections (left, right, main) of the normal rat models are respectively 2.9 GPa, 2.8 GPa, and 3.2 GPa. As expected, we find the radial stiffnesses increase for the normal hypoxic rat models compared to those of the normal rat models. However, we observe an unexpected decrease in the stiffness of the GM hypoxic rat models compared to that of the controls. We also observe uncertainties up to 20 % within a given population.

Fixed Specimens

The SOSs in the out-of-plane and in-plane directions for the three rat models are shown in Table 1. The standard deviations represent the spatial variation for the ROI of a single specimen. In general, we observe an increase in the SOS as we go from the normal to normal hypoxic to GM hypoxic rat models. The SOS for the normal rat model is greatest in the circumferential direction. The largest increase (≈ 135 m/s) in SOS between the normal and normal hypoxic rat models is in the radial direction. We observe increases in SOS in the longitudinal (≈ 100 m/s) and circumferential (≈ 150 m/s) directions between normal hypoxic and GM hypoxic.
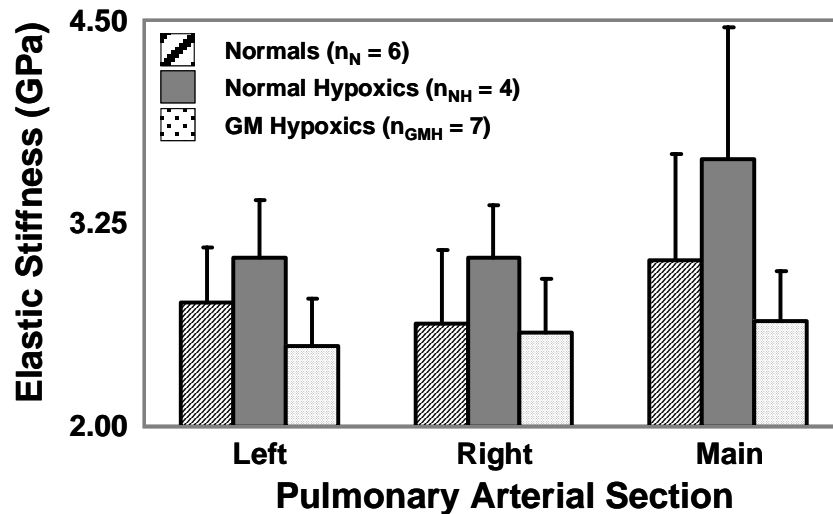
FIGURE 5. Radial stiffness (c_{11}) of the fresh PA walls (left branch, right branch, main trunk) for three rat model populations (normals, normal hypoxics, and genetically modified hypoxics).

TABLE 1. Speeds of sound (mean ± standard deviation) of fixed, main pulmonary artery from normal, normal hypoxic, and genetically modified rat models for out-of-plane and in-plane directions.

	Longitudinal (m/s)	Circumferential (m/s)	Radial (m/s)	Diagonal (m/s)
Normal	1613.1 ± 17.6	1648.1 ± 28.4	1612.8 ± 6.4	1601.4 ± 24.0
Normal Hypoxic	1627.7 ± 27.0	1639.7 ± 19.8	1747.9 ± 21.2	1633.0 ± 18.0
Genetically Modified Hypoxic	1731.1 ± 27.3	1791.1 ± 12.6	1812.3 ± 33.5	1684.3 ± 13.2

The SOSs shown in Table 1 were used to calculate the elastic stiffness coefficients according to Eqs. (3)-(6). As expected from the SOS measurements, the GM hypoxic rat model is the stiffest, with the possible exception for the off-diagonal element c_{12}. However, we have uncertainties of up to 30 % in c_{12} due to the estimated uncertainty in ϑ and ρ. The in-plane stiffnesses c_{11} and c_{22} are comparable for the normal and normal hypoxic models. However, the radial stiffness c_{33} of the normal hypoxic rat model is about 15 % larger than that of the normal rat model. We also observed an increase of approximately 10 % in the in-plane stiffnesses c_{11} and c_{22} when comparing the GM hypoxic rat model to the other two rat models. Differences in the mean stiffnesses are not tested for significance because there is only one rat specimen for each population type.

The results for the measurements of the fixed specimens do not appear at first to be consistent with the results of the fresh specimens. Here we are referring to the radial stiffness (c_{33}) of the main trunk. However, the measured values of the fixed specimens are consistent with the observation that some stiffening occurs as a result of the fixation process [8]. In addition, these values fall within the large uncertainties observed for the fresh specimens.
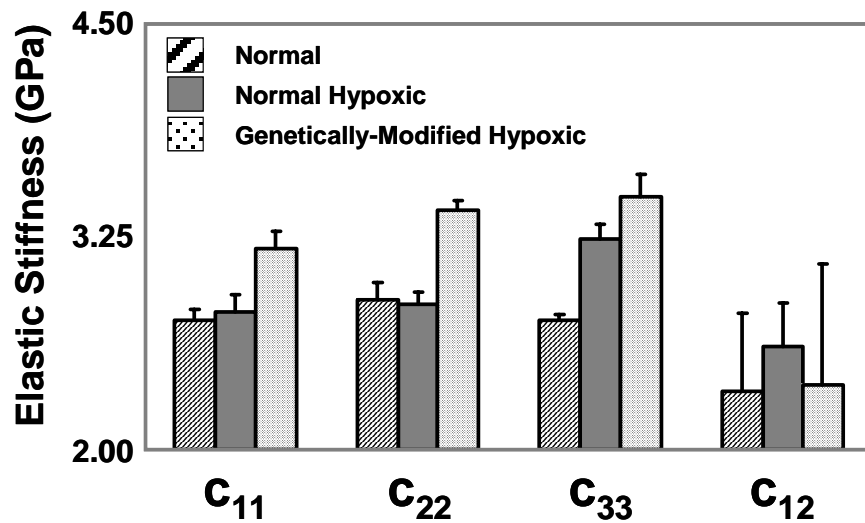
FIGURE 6. Out-of-plane (c_{33}) and in-plane (c_{11}, c_{22}, c_{12}) stiffnesses of fixed pulmonary arterial wall (main trunk only) for one specimen from each of the three rat model populations (normal, normal hypoxic, and genetically modified hypoxic).

CONCLUSION

We have performed high-frequency *in vitro* ultrasound measurements on fresh and fixed pulmonary arterial walls excised from normoxic and hypoxic rat models. The Long-Evans rat model was chosen for the study of pulmonary hypertension because it can be genetically modified to give the rat a greater propensity for developing hypertension. We approximated the elastic model of the medial layer of the pulmonary arterial wall as being transversely isotropic. For the fresh specimens, we observed an expected increase in the radial stiffness for the normal hypoxic rat models, but an unexpected decrease for the genetically modified rat models, when compared to the control rat model. The radial stiffness of the main trunk of the normal hypoxic model was on average 20 % greater than that of the control model. For the fixed specimens, we estimated both the out-of-plane and in-plane stiffnesses of the medial layer for a specimen from each rat model. The genetically modified rat model had the largest radial, longitudinal, and circumferential stiffnesses. Continuing efforts aim to understand the unexpected decrease in radial stiffness of the genetically modified hypoxic rat models, to assess the statistical significance of differences in elastic properties between the rat models, and to correlate changes in the elastic properties with tissue remodeling.

ACKNOWLEDGEMENTS

REFERENCES

1. Shandas, R., Weinberg, C., Ivy, D.D. et al., Circ. 104 (8), 908-913 (2001).
2. Fung, Y.C., "Effect of Stress on Tissue Growth", in Biomechanics: Mechanical Properties of Living Tissues, Springer-Verlag, New York, 1993, pp. 369-370.
3. Holzapfel, G.A., "Biomechanics of Soft Tissue", in Handbook of Material Behavior: Nonlinear models and Properties, edited by Jean Lemaitre, Academic Press, Boston, 2001, pp. 1049-1063.
4. Auld, B.A., Acoustic Fields and Waves in Solids Vol. 1, Robert E. Krieger Publishing Company, Malabar, Florida, 1990, pp. 396-398.
5. Sollish, B.D., "A Device for Measuring Ultrasonic Propagation Velocity in Tissue," in Ultrasonic Tissue Characterization II, edited by M. Linzer, U.S. Government Printing Office Spec. Publ. 525, Washington, D.C., 1979, pp. 53-56.
6. Del Grosso, V.A. and Mader, C.W., J. Acoust. Soc. Am. 52 (5 (Part 2)), 1442-1446 (1972).
7. Hoffmeister, B.K., Gehr, S.E., and Miller, J.G., J. Acoust. Soc. Am. 99 (6), 3826-3836 (1996); Kuo, P.-L., Li, P.-C., and Li, M.-L., Ultrasound Med. Biol. 27 (9), 1275-1284 (2001).
8. Hall, C.S., Dent, C.L., Scott, M.J. et al., IEEE Trans. Ultrason. Ferroelec. Freq. Contr. 47 (4), 1051-1058 (2000).